Journal of Medicinal Chemistry

pubs.acs.org/jmc

Article

Structure-Guided Optimization of Small-Molecule Folate Uptake Inhibitors Targeting the Energy-Coupling Factor Transporters

Alexander F. Kiefer,[‖] Spyridon Bousis,[‖] Mostafa M. Hamed,[‖] Eleonora Diamanti, Jörg Haupenthal, and Anna K.H. Hirsch*

Cite This: J. Med. Chem. 2022, 65, 8869–8880

Read Online

ACCESS | Metrics & More | Article Recommendations | Supporting Information

ABSTRACT: Here, we report on a potent class of substituted ureidothiophenes targeting energy-coupling factor (ECF) transporters, an unexplored target that is not addressed by any antibiotic in the market. Since the ECF module is crucial for the vitamin transport mechanism, the prevention of substrate uptake should ultimately lead to cell death. By utilizing a combination of virtual and functional whole-cell screening of our in-house library, the membrane-bound protein mediated uptake of folate could be effectively inhibited. Structure-based optimization of our hit yielded low-micromolar inhibitors, whereby the most active compounds showed in addition potent antimicrobial activities against a panel of clinically relevant Gram-positive pathogens without significant cytotoxic effects.

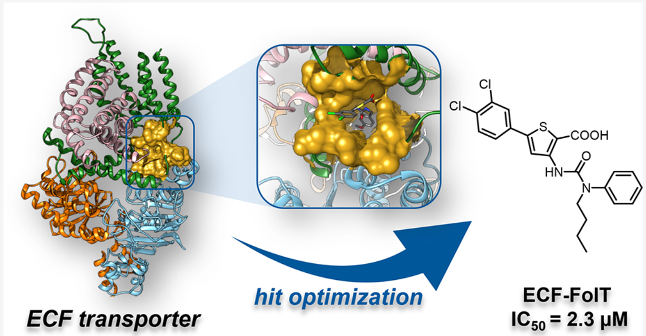

INTRODUCTION

Due to the increasing emergence of antimicrobial resistance (AMR) and the accompanying rise in morbidity and mortality rates, society is under immense pressure. In particular, multidrug resistant (MDR) pathogens, such as *Enterococcus faecium* or *Streptococcus pneumoniae*, were prioritized by the World Health Organization due to their difficult-to-treat behavior.[1] Such pathogens need to be tackled by drugs that address new biological targets, resulting in a novel mode of action.[2] The energy-coupling factor (ECF) transporters are transmembrane proteins widely distributed among Gram-positive bacteria. They are considered as highly attractive antimicrobial targets since they are required for the uptake of essential micronutrients, making them indispensable for both the growth and survival of bacteria.[3] These micronutrients are involved in cell metabolism and include water-soluble B-type vitamins such as folate,[4] panthothenate,[5] riboflavin,[6] and metal ions.[7,8] In general, ECF transporters belong to the family of the adenosine 5′-triphosphate (ATP)-binding cassette (ABC) transporters consisting of four domains.[9] Three of them form a complex that is called the ECF module, containing two nucleotide-binding domains (NBDs)—ECFA and ECFA′—that hydrolyze ATP,[10] as well as one transmembrane domain: ECF-T (or T-component). The fourth domain—ECF-S, the S-component—is a substrate-specific binding protein.[9] Different vitamins, for example, folate, are able to bind to dedicated S-components.[11] A common feature of ECF transporters is that the same ECF module can interact with various S-components, facilitating the uptake of a range of vitamins in the same cell.

We have recently reported a druggability assessment of the ECF-FolT as a novel and attractive antimicrobial target[12] along with a set of inhibitors as first tool compounds to explore the ECF transporters from a medicinal-chemistry perspective.[13]

Since previous studies were limited to tool compounds, we herein present the discovery of another chemical class that inhibits folate uptake mediated by the ECF-FolT transporter and its further biological evaluation. By combining structure-based virtual screening of our in-house small-molecule library and further examination of selected molecules *via* a *Lactobacillus casei* whole-cell assay, our endeavors revealed a highly promising hit compound bearing a ureidothiophene carboxylate core motif.[14] This compound served as an excellent starting point for further structure-based optimization. Synthesized derivatives and small molecules from our in-house library enabled a straightforward structure−activity relationship (SAR) study. Ultimately, the most active compounds were evaluated for their solubility and cytotoxicity and against several clinically relevant Gram-positive pathogens.

Received: December 10, 2021
Published: June 16, 2022

■ RESULTS AND DISCUSSION

To discover new inhibitors of the ECF transporters, we screened our in-house library consisting of more than 2000 small molecules by structure-based virtual screening. The first step was an *in silico* screening using docking calculations to select molecules with a predicted target affinity. For this purpose, we selected the P2 pocket—located inside the ECF-T module—that exhibits a good druggability score of 0.79 (Figure 1).[12] Since the ECF module is crucial for the vitamin transport mechanism, potential inhibitors should inhibit uptake of all substrates *via* ECF-T into the cell, ultimately leading to cell death.

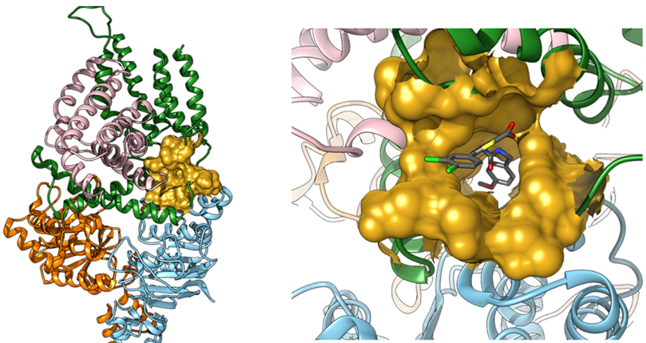

Figure 1. Cartoon representation of the group-II ECF-FolT transporter crystal structure responsible for folate uptake (PDB code 5JSZ).[11] ECFA, ECFA′, ECF-T, and ECF-S colored in orange, blue, green, and pink, respectively. P2 pocket depicted as a yellow-colored surface and ureidothiophene **1** in gray. Image generated with the CHIMERA software.[15]

The identified 111 virtual hits were then clustered according to their structural similarity, and the 22 top-ranked representatives were selected and evaluated in a *L. casei* cell-based assay.[14] Hit compound **1** displayed an inhibition of 54.3% at 50 μM, qualifying this class of substituted ureidothiophenes as a new ECF transporter inhibitor (Figure 2).

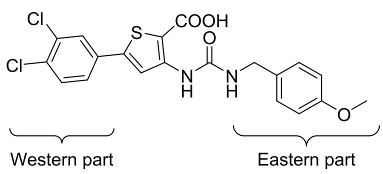

1 ECF-FolT inhibition at 50 μM = 54.3%

Figure 2. Hit compound **1** obtained from a combination of structure-based virtual and whole-cell screening.

For the library generation of ureidothiophenyl derivatives **1−48**, we used the combination of available in-house compounds (**1−21**, **24**, and **33−41**) and synthesized derivatives (**22−23**, **25−32**, and **42−48**), which can differ in the Western and Eastern part.[16−18] We commenced our synthesis from commercially available acetophenones ***I***. These were converted *via* a Vilsmeier−Haack-type reaction to the corresponding β-chloro-cinnamonitrile followed by cyclization utilizing methylthioglycolate, obtaining the thiophene anthranilic acids **II** (Scheme 1).[19] Subsequent saponification and treatment of the resulting acid **III** with the highly toxic phosgene afforded the thiaisatoic anhydrides **IV**.[20,21] Final

Scheme 1. Synthesis of 5-Aryl-3-ureidothiophene-2-carboxylic Acids 22−23 and 25−32[a]

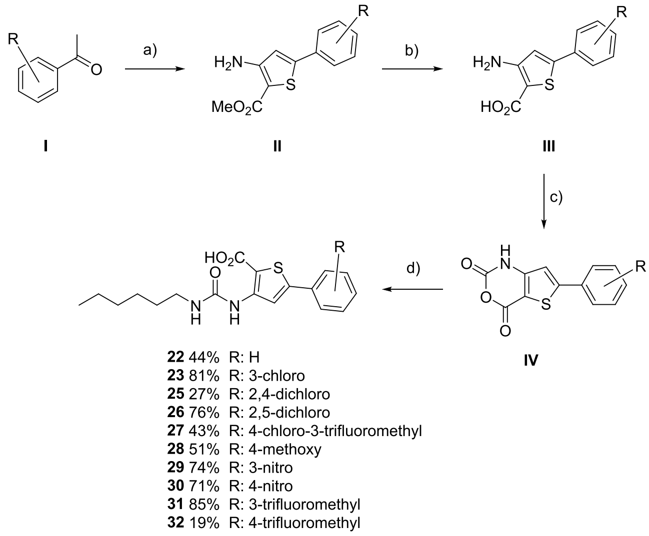

[a]Reagents and conditions: (a) (i) $POCl_3$, DMF, 50 °C to r.t.; (ii) $NH_2OH{\cdot}HCl$, up to 150 °C; (iii) methylthioglycolate, NaOMe, MeOH, reflux. (b) KOH, MeOH, THF, H_2O, reflux. (c) $COCl_2$, THF. (d) Amine, H_2O, 100 °C.[18]

conversion with a variety of amines gave rise to the 5-aryl-3-ureidothiophene-2-carboxylic acids **22**, **23**, and **25−32** in good yield.[17,18,22]

To get access to 4-aryl-3-ureidothiophene-2-carboxylic acids and their bioisosteric benzene analogue, we developed a robust and variable synthetic route that would allow us to substitute the urea moiety present in hit compound **1** with specific functional groups such as the corresponding amide and amine (Figure 3). We began our synthesis with the commercially available methyl 3-aminothiophene-2-carboxylate **V**, which was transformed into the corresponding urea derivative **43** with a yield of 51% using triphosgene (BTC) and hexylamine after saponification. To install the arylic moiety, **V** was first regioselectively brominated under acidic conditions.[23] Subsequent Suzuki cross-coupling yielded **VII**, **XIII**, and **XV**.[24,25] These intermediates represent extremely valuable precursors for further modification and allowed us to first isolate urea derivatives **47** and **48** in a two-step procedure. Installation of the appropriately truncated amine linker was achieved by sodium hydride mediated deprotonation of amine **VII** followed by alkylation with hexyl bromide. Final treatment with lithium hydroxide gave the desired acid **45** in 91% yield. The truncated amide linker was incorporated by reacting valeroyl chloride with precursor **VII** at a low temperature. At this point, the final saponification of **VIII** with lithium hydroxide led to the desired product **44** in 89% yield. We accessed the bioisosteric product **46** in the previously described manner by combining Suzuki cross-coupling between brominated methyl anthranilate **X** and (3,4-dichlorophenyl) boronic acid, subsequent saponification, and final BTC-mediated urea formation. Purification by preparative HPLC gave biphenyl urea derivative **46** in 38% yield.

Starting from hit compound **1**, we examined the structurally similar analogues available in our in-house library for extending the SAR and further hit optimization. First, we focused on the Eastern part of the molecule, where we varied the substituent R by introducing several mono- or di-substituted aliphatic,

https://doi.org/10.1021/acs.jmedchem.1c02114
J. Med. Chem. 2022, 65, 8869−8880

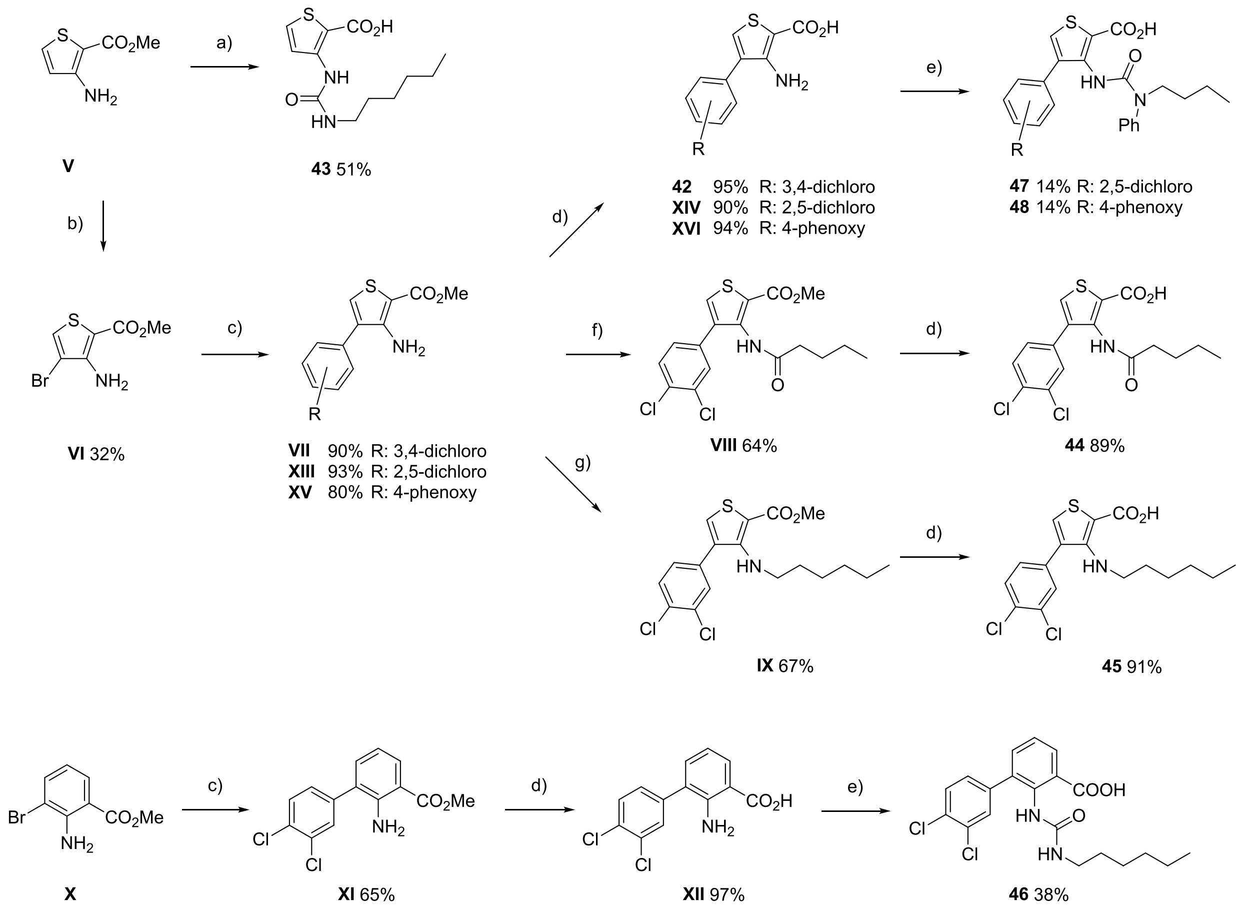

Figure 3. Synthesis of ureidothiophene-carboxylic acid derivatives **44**−**48**. Reagents and conditions: (a) (i) KOH, H_2O, 90 °C, 2 h; (ii) BTC, THF, 0 °C, 4 h; (iii) amine, THF, r.t., 24 h. (b) Br_2, AcOH, r.t., 24 h. (c) Boronic acid, cat. [$Pd(PPh_3)_4$], Na_2CO_3, dioxane/H_2O (4:1), 80 °C. (d) $LiOH{\cdot}H_2O$, THF/H_2O (4:1), 0 °C−r.t. (e) (i) BTC, THF, r.t., 2 h; (ii) amine, THF/H_2O (1:1), r.t., 24 h. (f) DIPEA, valeroyl chloride, −20 °C−r.t., 12 h. (g) NaH, hexylbromide, DMF, 12 h.

aromatic, and heterocyclic groups (Table 1). All compounds were tested for their proportional inhibition of the radiolabeled folic acid uptake into *L. casei* cells. For all compounds showing more than 70% inhibition at 50 μM, we additionally determined their half-maximal inhibitory concentration (IC_{50}).

Variation of the Eastern part of the molecule revealed that increasing the size of the aliphatic side chain enhances the activity (**3**, **4**, and **5**) compared to the unsubstituted urea motif present in **2**. Adding a polar carboxylic group (**4** *vs* **6**) causes a drop in activity. Introducing a directly linked phenyl ring (**7**) significantly boosts the activity, and having a further spacer between the urea and the phenyl ring (**8** and **9**) almost retains the activity. Replacing the phenyl ring (**8**) by a pyridyl (**10**, **11**, and **12**) results in generally less potent derivatives. The position of the heteroatom does not seem to further affect the activity. Additionally, the activity was influenced by having two aromatic groups or one aromatic and one aliphatic group in addition to the presence or absence of a spacer in the disubstituted derivatives. Accordingly, adding a methyl as a second substituent besides the phenyl (**13**) decreases the activity, while further elongation to an ethyl (**14**) or a butyl (**15**) boosts the activity. Keeping the butyl group constant and introducing a spacer to the phenyl result in a further decrease in activity (**16** and **17**). Keeping the benzyl group constant while adding an extra methyl (**18**) or ethyl (**19**) results in an enhancement in activity relative to the benzyl alone (**8**) with both compounds being equipotent. Replacing the alkyl groups with a phenyl ring (**20**) boosts the activity, while having another benzyl substituent (**21**) further decreases the activity.

For the next set of modifications, we maintained the Eastern part of compounds **5** and **19** as they were among the most potent derivatives, and various structurally related analogues were available in our in-house library. This set of modifications included changes in the Western part of the molecule (Table 2) besides studying the influence of the different regioisomers on activity (Table 3).

Modifications of the Western part showed that the dichlorinated derivatives are more potent than the monochlorinated ones. Among the created derivatives, 2,5-dichlorophenyl (**26**) and 3,4-dichlorophenyl (**5**) were the most potent ones. Having in mind the relative potencies of compounds **5** and **19**, we compared the different substituents in *para* position. The results revealed that the NO_2 group (**30**) showed the highest increase in activity followed by OCF_3 (**36**) > Br (**34**) > Me (**35**) > CF_3 (**32**), while the CN (**37**) was the least potent. Among the 3,4 di-substituted derivatives, the dichloro was always more potent than the CF_3 congener (**5** *vs* **27**). Interestingly, further extension with a phenoxy (**38**) is tolerated and results in enhanced activity.

As a next step, we wanted to compare the impact of the different regioisomers on activity (Table 3). This revealed that switching the positions of the carboxylic and the urea groups results in a complete loss in activity (**5** *vs* **39**). Interestingly, the 2,3,4-substitution pattern is more favorable than 2,3,5 and

https://doi.org/10.1021/acs.jmedchem.1c02114
J. Med. Chem. 2022, 65, 8869−8880

Table 1. Eastern Part Modifications with Their % Inhibition and IC_{50} Values against ECF-FolT[b]

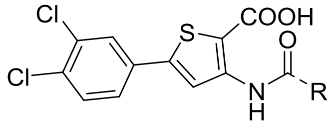

compound	R	% inhibition ECF-FolT at 50 μM	IC_{50} (μM)
1	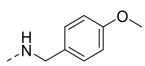	54.3 ± 1.4	n.d.[a]
2		42.4 ± 0.7	n.d.
3	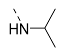	39.3 ± 18.0	n.d.
4	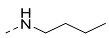	61.9 ± 21.8	n.d.
5	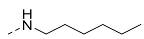	72.2 ± 7.3	28.5 ± 9.9
6	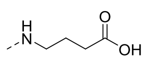	0.2 ± 12.9	n.d.
7	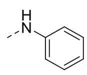	86.8 ± 5.4	14.4 ± 6.3
8	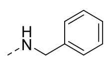	71.1 ± 0.9	17.8 ± 7.7
9	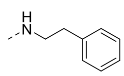	91.7 ± 1.7	15.3 ± 7.5
10	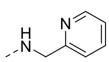	59.0 ± 9.2	n.d.
11	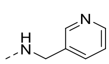	58.0 ± 20.2	n.d.

compound	R	% inhibition ECF-FolT at 50 μM	IC_{50} (μM)
12	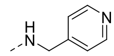	54.0± 9.1	n.d.
13	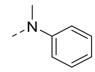	71.5 ± 2.8	23.0 ± 8.9
14	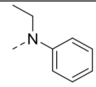	83.2 ± 1.8	10.5 ± 0.5
15	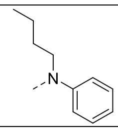	99.6 ± 0.6	2.35 ± 0.80
16	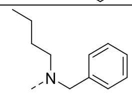	42.5 ± 15.3	n.d.
17	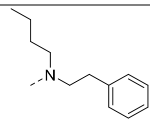	57.8 ± 13.7	n.d.
18	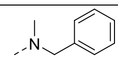	86.9 ± 3.9	10.0 ± 0.4
19	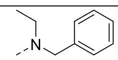	89.4 ± 1.4	11.4 ± 0.9
20	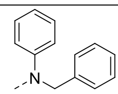	91.3 ± 3.3	2.94 ± 0.02
21	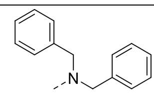	85.1 ± 4.3	24.0 ± 11.5

[a]n.d. = not determined. [b]The data shown were obtained from two independent experiments. Each experiment was performed in duplicate.

enhanced the activity (**5** *vs* **40**). Flipping the carboxylic with the urea in the 2,3,4 pattern turned out again not to be beneficial (**40** *vs* **41**).

A final set of modifications was performed based on the more potent regioisomer **40** where we evaluated the importance of the urea and the main thiophenyl core in addition to the effect of truncation (Table 4). It was clearly seen that any truncation of the Eastern or the Western part leads to a significant loss of activity (*cf.* **42** and **43**). To explore the importance of the urea linker, we replaced it with an amide (**44**) and an amine (**45**). Although the urea remained the most potent, the amine (**45**) was just slightly less potent, while the amide (**44**) showed a more pronounced decrease in activity. Finally, scaffold hopping was done by replacing the main thiophenyl core with a phenyl ring (**46**). Interestingly, this was acceptable with only a slight decrease in activity.

Based on the results of all the modifications tested, we finally combined the best features. We used the most potent Eastern part in compound **15**, which incorporates a phenyl and a butyl residue. For the Western part, we chose phenoxy-phenyl and 2,5-dichlorophenyl residues as incorporated in the most potent compounds **38** and **26**, respectively. Combination of the Eastern and the Western parts using the more potent 2,3,4-substitued core resulted in compounds **47** and **48**. While merged 2,5-dichlorophenyl compound **47** did not show the desired enhancement in activity, this came true for phenoxy-phenyl derivative **48**, which revealed an excellent folate uptake inhibition with an IC_{50} value of 3.9 μM. This could in part be due to the 2,3,4-substitiuted core having a different SAR requirement than the 2,3,5-substituted core from which we adopted the SAR.

The superb inhibition of **15** and **48** encouraged us to further evaluate their minimal inhibitory concentrations (MICs) against a broad panel of clinically relevant Gram-positive pathogens, along with their solubility and cytotoxic effects on human liver cancer cells (HepG2), human embryonic kidney

Table 2. Western Part Modifications with Their % Inhibition and IC_{50} Values against ECF-FolT[b]

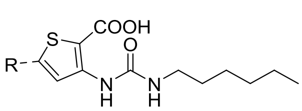

A

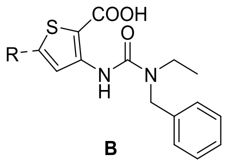

B

compound	core	R	% inhibition ECF-FolT at 50 µM	IC_{50} (µM)
22	**A**	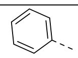	25.1 ± 3.7	n.d.[a]
23	**A**	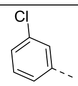	36.2 ± 2.6	n.d.
24	**A**	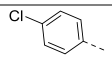	27.2 ± 1.7	n.d.
25	**A**	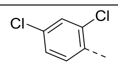	67.9 ± 0.5	n.d.
26	**A**	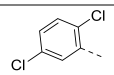	93.4 ± 4.2	21.8 ± 0.1
27	**A**	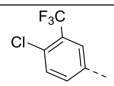	59.0 ± 5.0	n.d.
28	**A**	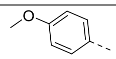	12.1 ± 10.6	n.d.
29	**A**	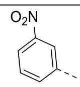	65.3 ± 9.6	43.3 ± 1.5
30	**A**	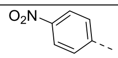	82.1 ± 4.6	25.1 ± 2.2
31	**A**	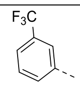	52.3 ± 0.8	n.d.
32	**A**	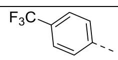	27.1 ± 1.8	n.d.
33	**B**	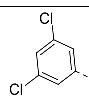	22.0 ± 14.8	n.d.
34	**B**	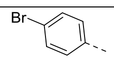	52.3 ± 1.9	n.d.
35	**B**	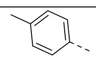	38.9 ± 2.7	n.d.
36	**B**	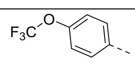	67.2 ± 1.7	n.d.
37	**B**	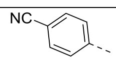	18.3± 0.3	n.d.
38	**B**	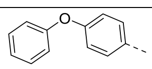	97.0 ± 0.8	10.1 ± 1.2

[a]n.d. = not determined. [b]The data shown were obtained from two independent experiments. Each experiment was performed in duplicate.

Table 3. The Different Regioisomers with Their % Inhibition and IC_{50} Values against ECF-FolT[b]

compound	structure	% inhibition ECF-FolT at 50 µM	IC_{50} (µM)
5	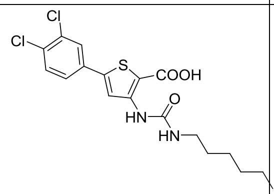	72.2 ± 7.3	28.5 ± 9.9
39	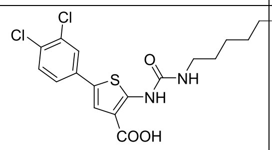	17.9 ± 18.3	n.d.[a]
40	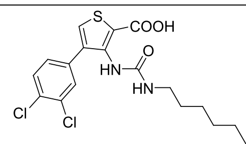	90.6 ± 1.8	6.0 ± 2.3
41	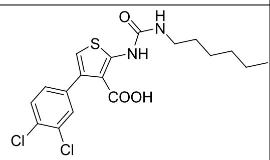	87.5 ± 4.6	18.5 ± 0.4

[a]n.d. = not determined. [b]The data shown were obtained from two independent experiments. Each experiment was performed in duplicate.

cells (HEK293), and adenocarcinoma human alveolar basal epithelial cells (A549) (Table 5). Notably, while both compounds did not show drastic cytotoxic effects in HepG2 and A549 cells, a moderate decrease in cell viability was revealed for HEK293 cells. Both **15** and **48** showed good kinetic solubility[26], indicating adequate access to the envisaged P2 pocket of the transmembrane protein since further cell uptake is not necessary. Unfortunately, we observed only a slight antimicrobial effect of **15** and **48** for *Staphylococcus aureus*, suggesting that *S. aureus* does not necessarily rely on the folate uptake and predominantly obtains it directly via the biosynthesis.[12,27] Beyond that, compound **48** exhibited a good activity of 16 and 8 μM for both wild-type *E. faecium* and the vancomycin-resistant *E. faecium*, whereas **15** showed an even stronger inhibition of the wild-type and the antibiotic-resistant strain, revealing an MIC value of 2 μM. Also the susceptible *S. pneumoniae* strain could be effectively treated by our optimized compounds, showing an MIC value of 2 (**15**) and 4 μM (**48**), whereas compound **48** lost its effect on the penicillin-resistant strain with 16 μM. The latter displayed only mild cytotoxic effects at an IC_{50} of 57 μM. Most interestingly, ureidothiophene **15** inhibits the penicillin-resistant *S. pneumoniae* strain with an MIC value of 0.5 μM while only showing an insignificant cytotoxic effect. These findings make ureidothiophene **15** an excellent candidate for further development as an antibiotic, showing a superb therapeutic window while presenting a novel mode of action.

https://doi.org/10.1021/acs.jmedchem.1c02114
J. Med. Chem. 2022, 65, 8869−8880

Table 4. Variable Modifications and Merged Derivatives on the More Potent Regioisomer with Their % Inhibition and IC_{50} Values against ECF-FolT[d]

compound	structure	% inhibition ECF-FolT at 50 µM	IC_{50} (µM)
42	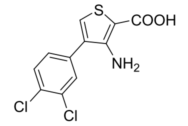	n.i.[a]	n.d.[b]
43	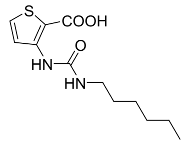	n.i.	n.d.
44	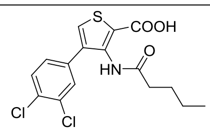	31.8 ± 0.7	n.d.
45	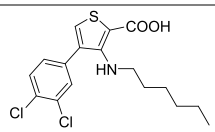	95.2± 3.3	n.d.[c]
46	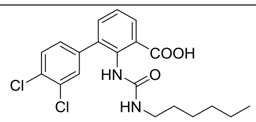	65.4± 0.7	n.d.
47	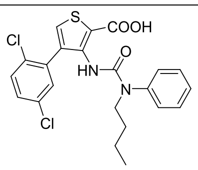	73.4 ± 1.1	17.0 ± 6.3 µM
48	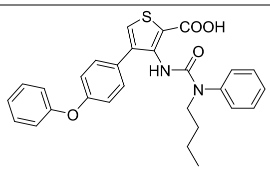	100.4 ± 1.4	3.9 ± 0.5

[a]n.i. = <10% inhibition. [b]n.d. = not determined. [c]Compound decomposed under assay conditions. [d]The data shown were obtained from two independent experiments. Each experiment was performed in duplicate.

■ CONCLUSIONS

We discovered a potent class of substituted ureidothiophenes targeting ECF transporters, an unexplored target that is not addressed by any antibiotic in the market. Starting from an in-house library screening hit, an extensive SAR study was done by exploring the Eastern and Western parts of the molecule as well as different possible regioisomers. This finally led to two highly potent ECF inhibitors, **15** and **48**, revealing single-digit micromolar inhibition. Beyond the superb on-target activity of those two molecules, potent antibacterial activities against a panel of Gram-positive clinically relevant strains were observed, first and foremost the penicillin-resistant *S. pneumoniae* inhibition at 0.5 μM. Both frontrunners only showed mild cytotoxic effects on human cell lines, paving the way for the development of further ureidothiophene-based antibacterial drugs targeting ECF-transporters.

Table 5. Antibacterial Profiles, Cytotoxicity, and Kinetic Solubility of Compounds 15 and 48[c]

strain	compound 15	compound 48
	MIC [μM]	
Enterococcus faecium DSM-20477	8	16
VR-*Enterococcus faecium* DSM-17050[a]	2	8
Streptococcus pneumoniae DSM-20566	2	4
PR-*Streptococcus pneumoniae* DSM-11865[b]	0.5	16
Staphylococcus aureus Newman	23	16
	IC_{50} [μM]	
HepG2	95.6 ± 9.4	57.0 ± 0.9
HEK293	52.5 ± 2.7	25.5 ± 2.9
A549	>100	49.3 ± 2.6
	Kinetic solubility S_{kin} [μM]	
	106.6 ± 1.9	>200

[a]VR: vancomycin-resistant. [b]PR: penicillin-resistant. [c]The MIC determinations were performed in three independent experiments, each in duplicate.

■ EXPERIMENTAL SECTION

Chemistry. All air- or moisture-sensitive reactions were carried out in dried glassware (>100 °C) under an atmosphere of nitrogen or argon. Dried solvents were distilled before use. Analytical TLC was performed on precoated silica gel plates (Macherey-Nagel, Polygram SIL G/UV254). Visualization was accomplished with UV-light, $KMnO_4$, or a ceric ammonium molybdate chamber. The products were purified by flash chromatography on silica gel columns (Macherey-Nagel 60, 0.04−0.063 mm). Preparative high-performance liquid chromatography (HPLC) was performed on a Waters Autopurifier System (APS) with a Phenomenex Gemini C18 column (250 × 4.6 mm, particle size 5 μm) as an analytical column for method development and a Phenomenex Gemini C18 column (250 × 19 mm, particle size 5 μm) for preparative separation. Detection was performed using a mass trigger. ^{1}H and ^{13}C spectra were recorded with a Bruker Fourier Spectrometer [300 MHz (^{1}H), 75 MHz (^{13}C)] or a Bruker AV 500 [500 MHz (^{1}H), 126 MHz (^{13}C)] spectrometer in $CDCl_3$, DMSO-d_6, or MeOH-d_4 unless otherwise specified. Chemical shifts are given in parts per million (ppm) and referenced against the residual proton or carbon resonances of the >99% deuterated solvents as internal standard. Coupling constants (J) are given in hertz (Hz). Data are reported as follows: chemical shift, multiplicity (s = singlet, d = doublet, t = triplet, q = quartet, m = multiplet, dd = doublet of doublets, dt = doublet of triplets, br = broad, and combinations of these) coupling constants, and integration. NMR spectra were evaluated using ACDLabs 2019. Liquid chromatography−mass spectrometry (LC−MS) was performed on a LC−MS system consisting of a Dionex UltiMate 3000 pump, autosampler, column compartment, detector (Thermo Fisher Scientific, Dreieich, Germany), and ESI quadrupole MS (MSQ Plus or ISQ EC, Thermo Fisher Scientific, Dreieich, Germany). High-resolution mass was determined by LC−MS/MS using the Thermo Scientific Q Exactive Focus Orbitrap LC−MS/MS system. The purity of the final compounds was determined by LC−MS using a gradient with (A) H_2O + 0.1% FA to (B) ACN + 0.1% FA at a flow rate of 600 μL/min and 45 °C. The gradient was initiated by a 1 min isocratic step at 5% B followed by an increase to 99% B in 15 min to end up with a 5 min step at 99% B before re-equilibration under the initial conditions. The purity of the final compounds was determined by using the area percentage method on the UV trace recorded at a wavelength of 254 nm and found to be >95%.

General Procedure for the Synthesis of 5-Aryl-3-amino-2-carboxylic Acid Methylester (II).[19] $POCl_3$ (26.1 g, 0.17 mol) was added dropwise to DMF (24.9 g, 0.34 mol) while maintaining the

https://doi.org/10.1021/acs.jmedchem.1c02114
J. Med. Chem. 2022, 65, 8869−8880

temperature below 25 °C (cooling in ice bath) and stirred for an additional 15 min. The acetophenone **I** (85.0 mmol) was added slowly, and the temperature was kept between 40 and 60 °C. After complete addition, the mixture was stirred for 30 min at room temperature. Hydroxylamine hydrochloride (23.6 g, 0.34 mol) was carefully added portion-wise, and the reaction was stirred for an additional 30 min without heating. After cooling to room temperature, the mixture was poured into ice water (300 mL). The precipitated β-chloro-cinnamonitrile was collected by filtration, washed with H_2O (2 × 50 mL), and dried under reduced pressure over $CaCl_2$ in a vacuum desiccator. In the next step, sodium (1.93 g, 84.0 mmol.) was dissolved in MeOH (85 mL), and methylthioglycolate (6.97 g, 65.6 mmol) was added to the stirred solution. The β-chloro-cinnamonitrile (61.1 mmol) was added, and the mixture was heated to reflux for 30 min. After cooling to room temperature, the mixture was poured into ice water (300 mL). The precipitated solid was collected by filtration, washed with H_2O (2 × 50 mL), and dried under reduced pressure over $CaCl_2$ in a vacuum desiccator. If necessary, recrystallization was performed from EtOH.

General Procedure for the Synthesis of 5-Aryl-3-amino-2-carboxylic Acid (III). The 5-aryl-3-amino-2-carboxylic acid methyl ester **II** (16.6 mmol) was added to a solution of KOH (60 mL, 0.6 M in H_2O) and MeOH (60 mL). The mixture was heated to reflux for 3 h, concentrated, and washed with EtOAc (2 × 50 mL). The aqueous layer was cooled with ice and acidified with a saturated aqueous solution of $KHSO_4$. The precipitated solid was collected by filtration, washed with H_2O (2 × 30 mL), and dried under reduced pressure over $CaCl_2$ in a vacuum desiccator.

General Procedure for the Synthesis of 5-Aryl-2-thiaisatoic-anhydride (IV).[20,21] To a solution of the 5-aryl-3-amino-2-carboxylic acid (**III**) (5.28 mmol) in THF (50 mL), a solution of phosgene (6.10 mL, 20 wt % in toluene, 11.6 mmol) was added dropwise over a period of 30 min. The reaction mixture was stirred at room temperature for 2 h followed by the addition of a saturated aqueous solution of $NaHCO_3$ (30 mL) and H_2O (50 mL). The resulting mixture was extracted with EtOAc/THF (1:1, 3 × 100 mL). The organic layer was washed with brine (100 mL), dried ($MgSO_4$), filtered, and concentrated. The crude material was suspended in a mixture of *n*-hexane/EtOAc (2:1, 50 mL) heated to 50 °C and after cooling to room temperature separated *via* filtration.

Caution: Phosgene is a highly toxic, irritating, and corrosive gas. Inhalation can cause fatal respiratory damage. Wear chemical splash goggles and impermeable gloves. Containers of phosgene solutions should be stored in secondary corrosion-resistant and lightning-resistant containers in a ventilated fridge at 2−8 °C. Keep away from water. Cylinder temperature should never exceed 51 °C. Before opening or entry into equipment that has contained phosgene, purge with a dry inert gas such as N_2. Never work alone with phosgene. If phosgene is released, immediately leave the area until the severity of the release is determined. Phosgene wastes can best be handled through caustic scrubbing in packed columns or by scrubbing in towers with activated carbon and water. Phosgene or aqueous phosgene wastes should never be disposed without prior alkaline neutralization.

General Procedure for the Synthesis of 5-Aryl-3-ureido-thiophene-2-carboxylic Acid 22−23 and 24−32.[22] The 5-aryl-2-thiaisatoic-anhydride (**IV**) (0.46 mmol) was suspended in water (7.5 mL), and the appropriate amine (4.60 mmol) was added. The reaction mixture was stirred, heated to 100 °C, and then cooled to room temperature. The reaction mixture was poured into a mixture of concentrated HCl and ice (1:1) and extracted with EtOAc/THF (1:1, 60 mL). The organic layer was washed with aqueous HCl (2 M) followed by brine (2 × 50 mL), dried ($MgSO_4$), filtered, and concentrated. The crude material was suspended in a mixture of *n*-hexane/EtOAc (2:1, 20 mL) heated to 50 °C and after cooling to room temperature separated *via* filtration.

*3-(3-Hexylureido)-5-phenylthiophene-2-carboxylic Acid (**22**).* The title compound was prepared from acetophenone according to the general procedure to yield **22** (0.13 g, 0.37 mmol, 44%) as a yellow, amorphous powder. ^{1}H NMR (300 MHz, DMSO-d_6): δ = 0.86 (t, *J* = 6.9 Hz, 3H), 1.26−1.45 (m, 8H), 3.09 (dt, 2H), 7.37−7.48 (m, 3H), 7.66 (m, 3H), 8.29 (s, 1H), 9.23 (s, 1H), 13.05 (br. s, 1H). ^{13}C NMR (75 MHz, DMSO-d_6) δ = 13.9, 22.1, 26.1, 29.4, 31.0, 39.3, 106.2, 117.9, 125.6, 129.1, 129.3, 132.8, 146.5, 146.9, 153.7, 164.8. HRMS (ESI−) *m*/*z* calculated for $C_{18}H_{21}N_2O_3S$ [M−H]$^-$ 345.1278; found, 345.1271.

*5-(3-Chlorophenyl)-3-(3-hexylureido)thiophene-2-carboxylic Acid (**23**).* The title compound was prepared from 3-chloro-acetophenone according to the general procedure to yield **23** (0.23 g, 0.59 mmol, 81%) as a yellow, amorphous powder. ^{1}H NMR (300 MHz, DMSO-d_6): δ = 0.86 (t, *J* = 6.9 Hz, 3H), 1.26−1.45 (m,8H), 3.09 (dt, *J* = 6.7, 5.7, 2H), 7.44−7.51 (m, 2H), 7.59−7.64 (m, 2H), 7.68 (s, 1H), 8.32 (s, 1H), 9.30 (s, 1H), 13.14 (br. s, 1H). ^{13}C NMR (75 MHz, DMSO-d_6) δ =13.9, 22.1, 26.1, 29.4, 31.0, 39.3, 107.0, 118.9, 124.4, 125.1, 128.8, 131.2, 134.0, 134.9, 144.8, 146.3, 153.8, 164.7. HRMS (ESI−) *m*/*z* calculated for $C_{18}H_{20}ClN_2O_3S$ [M−H]$^-$ 379.0889; found, 379.0883.

*5-(2,4-Dichlorophenyl)-3-(3-hexylureido)thiophene-2-carboxylic Acid (**25**).* The title compound was prepared from 2,4-dichloro-acetophenone according to the general procedure to yield **25** (0.05 g, 0.13 mmol, 27%) as a yellow, amorphous powder. ^{1}H NMR (300 MHz, DMSO-d_6): δ = 0.86 (t, *J* = 6.9, 1.20−1.35 (m, 6H), 1.38−1.46 (m, 2H), 3.04−3.1 (m, 2H), 7.52 (dd, *J* = 8.5, 2.1, 1H), 7.65 (1H), 7.66 (d, *J* = 8.5, 1H), 7.79 (d, *J* = 2.1, 1H), 8.27 (s, 1H), 9.30 (s, 1H), 13.20 (br. s., 1H). ^{13}C NMR (75 MHz, DMSO-d_6) δ = 13.9, 22.1, 26.1, 29.4, 31.0, 39.2, 108.1, 122.74, 128.1, 130.1, 130.6, 132.1, 132.3, 134.1, 141.6, 145.3, 153.8, 164.6. HRMS (ESI−) *m*/*z* calculated for $C_{18}H_{19}Cl_2N_2O_3S$ [M−H]$^-$ 413.0499; found, 413.0493.

*5-(2,5-Dichlorophenyl)-3-(3-hexylureido)thiophene-2-carboxylic Acid (**26**).* The title compound was prepared from 2,5-dichloro-acetophenone according to the general procedure to yield **26** (0.15 g, 0.36 mmol, 76%) as a yellow, amorphous powder. ^{1}H NMR (300 MHz, DMSO-d_6): δ = 0.85 (t, *J* = 6.7, 1H), 1.20−1.35 (m, 6H), 1.40−1.46 (m, 2H), 3.04−3.1 (m, 2H), 7.50 (dd, *J* = 8.6, 2.4, 1H), 7.61−7.67 (m, 3H), 8.27 (s, 1H), 9.30 (s, 1H), 13.21 (br. s., 1H). ^{13}C NMR (75 MHz, DMSO-d_6) δ = 13.9, 22.1, 26.1, 29.4, 31.0, 32.2, 108.4, 123.1, 129.9, 130.1, 130.3, 132.2, 132.3, 133.3, 141.1, 145.2, 153.8, 164.6. HRMS (ESI−) *m*/*z* calculated for $C_{18}H_{19}Cl_2N_2O_3S$ [M−H]$^-$ 413.0499; found, 413.0492.

*5-(4-Chloro-3-(trifluoromethyl)phenyl)-3-(3-hexylureido)-thiophene-2-carboxylic Acid (**27**).* The title compound was prepared from 4-chloro-3-trifluoromethyl-acetophenone according to the general procedure to yield **27** (0.08 g, 0.19 mmol, 43%) as a yellow, amorphous powder. ^{1}H NMR (300 MHz, DMSO-d_6): δ = 0.86 (t, *J* = 6.9, 3H),1.19−1.32 (m, 6H), 1.39−1.46 (m, 2H), 3.05−3.11 (m, 2H), 7.65 (m, 1H), 7.79 (m, 1H), 7.95−7.97 (m, 2H), 8.38 (s, 1H), 9.30 (s, 1H), 13.23 (br. s., 1H). ^{13}C NMR (75 MHz, DMSO-d_6) δ = 13.9, 22.1, 26.1, 29.4, 31.0, 107.6, 119.6, 124.4 (q, *J* = 5.20 Hz), 127.40 (q, *J* = 30.50 Hz), 130.9, 131.1, 132.4, 132.6, 143.4, 146.3, 153.7, 164.6. HRMS (ESI−) *m*/*z* calculated for $C_{19}H_{19}ClF_3N_2O_3S$ [M−H]$^-$ 447.0762; found, 447.0766.

*3-(3-Hexylureido)-5-(4-methoxyphenyl)thiophene-2-carboxylic Acid (**28**).* The title compound was prepared from 4-methoxy-acetophenone according to the general procedure to yield **28** (0.10 g, 0.28 mmol, 51%) as a yellow, amorphous powder. ^{1}H NMR (300 MHz, DMSO-d_6): δ = 0.87 (t, *J* = 6.9, 3H), 1.27−1.45 (m, 8H), 3.08 (dt, *J* = 6.5, 5.7, 2H), 3.8 (s, 3H), 7.02 (dd, *J* = 8.9, 2.1, 2H), 7.59 (dd, *J* = 8.89, 2.1, 2H), 8.17 (s, 1H), 9.31 (s, 1H), 12.94 (br.s, 1H). ^{13}C NMR (75 MHz, DMSO-d_6) δ = 13.9, 22.1, 26.1, 29.4, 31.0, 39.3, 55.3, 105.1, 114.7, 116.7, 125.5, 127.1, 146.6, 147.1, 153.8, 160.0, 164.8. HRMS (ESI−) *m*/*z* calculated for $C_{19}H_{23}N_2O_4S$ [M−H]$^-$ 375.1384; found, 375.1379.

*3-(3-Hexylureido)-5-(3-nitrophenyl)thiophene-2-carboxylic Acid (**29**).* The title compound was prepared from 3-nitro-acetophenone according to the general procedure to yield **29** (0.15 g, 0.39 mmol, 74%) as a yellow, amorphous powder. ^{1}H NMR (300 MHz, DMSO-d_6): δ = 0.86 (t, *J* = 6.8, 3H), ,1.27−1.32 (m, 6H), 1.40−1.46 (m, 2H), 3.06−3.12 (m, 2H), 7.67 (br. t., 1H), 7.74 (t, *J* = 8.0, 1H), 8.11 (d, *J* = 8.5, 1H), 8.23 (dd, *J* = 8.2, 1.5, 1H), 8.35 (t, *J* = 1.9, 1H), 8.42 (s, 1H), 9.30 (s, 1H), 13.20 (br. s., 1H). ^{13}C NMR (75 MHz, DMSO-

https://doi.org/10.1021/acs.jmedchem.1c02114
J. Med. Chem. 2022, 65, 8869−8880

d_6) δ = 13.9, 22.1, 26.1, 29.4, 31.0, 40, 107.6, 119.6, 119.8, 123.4, 131.0, 131.9, 134.3, 143.7, 146.3, 148.4, 153.7, 164.6. HRMS (ESI−) *m/z* calculated for $C_{18}H_{20}N_3O_5S$ [M−H]$^-$ 390.1129; found, 390.1124.

*3-(3-Hexylureido)-5-(4-nitrophenyl)thiophene-2-carboxylic Acid (**30**).* The title compound was prepared from 4-nitro-acetophenone according to the general procedure to yield **30** (0.14 g, 0.37 mmol, 71%) as a yellow, amorphous powder. ^{1}H NMR (300 MHz, DMSO-d_6): δ = 0.87 (t, *J* = 6.8, 3H), 1.20−1.35 (m, 6H), 1.40−1.46 (m, 2H), 3.06−3.12 (m, 2H), 7.67 (m, 1H), 7.93 (d, *J* = 8.9, 2H), 8.26 (d, *J* = 8.9, 2H), 8.46 (s, 1H), 9.30 (s, 1H), 13.1 (br. s., 1H). ^{13}C NMR (75 MHz, DMSO-d_6) δ = 13.9, 22.1, 26.1, 29.4, 31.0, 39.3, 108.6, 120.3, 124.5, 126.6, 138.9, 143.6, 146.3, 147.1, 153.7, 164.6. HRMS (ESI−) *m/z* calculated for $C_{18}H_{20}N_3O_5S$ [M−H]$^-$ 390.1129; found, 390.1121.

*3-(3-Hexylureido)-5-(3-(trifluoromethyl)phenyl)thiophene-2-carboxylic Acid (**31**).* The title compound was prepared from 3-trifluoromethyl-acetophenone according to the general procedure to yield **31** (0.16 g, 0.41 mmol, 85%) as a yellow, amorphous powder. ^{1}H NMR (300 MHz, DMSO-d_6): δ = 0.87 (t, *J* = 6.9, 3H), 1.22−1.33 (m, 6H), 1.40−1.46 (m, 2H), 3.09 (q, *J* = 6.6, 2H), 7.64−7.79 (m, 3H), 7.92 (s, 1H), 7.98 (d, *J* = 7.6, 1H), 8.38 (s, 1H), 9.31 (s, 1H), 13.20 (br. s., 1H). ^{13}C NMR (75 MHz, DMSO-d_6) δ = 13.9, 22.1, 26.1, 29.4, 31.0, 107.3. 119.2, 121.81 (q, *J* = 3.72 Hz), 122.0, 125.5 (q, *J* = 3.23 Hz), 129.7, 130.1 (q, *J* = 31.30 Hz), 130.6, 133.9, 144.6, 146.3, 153.8, 164.6. 164.6. HRMS (ESI−) *m/z* calculated for $C_{19}H_{20}F_3N_2O_3S$ [M−H]$^-$ 413.1152; found, 413.1147.

*3-(3-Hexylureido)-5-(4-(trifluoromethyl)phenyl)thiophene-2-carboxylic Acid (**32**).* The title compound was prepared from 4-trifluoromethyl-acetophenone according to the general procedure to yield **32** (0.04 g, 0.09 mmol, 19%) as a yellow, amorphous powder. ^{1}H NMR (300 MHz, DMSO-d_6): δ = 0.86 (t, *J* = 6.8, 3H), 1.24−1.46 (m, 8H), 3.09 (q, *J* = 6.8, 2H), 7.66 (m, 1H), 7.79 (d, *J* = 8.5, 2H), 7.89 (d, *J* = 8.2, 2H), 8.41 (s, 1H), 9.33 (s, 1H), 12.94 (br. s., 1H). ^{13}C NMR (75 MHz, DMSO-d_6) δ = 13.9, 22.1, 26.1, 29.4, 31.0, 107.3. 119.4, 122.2, 126.2 (q, *J* = 3.70 Hz), 126.3, 128.9 (q, *J* = 32.04 Hz), 136.6, 144.5, 146.3, 153.8, 164.7. HRMS (ESI+) *m/z* calculated for $C_{19}H_{22}F_3N_2O_3S$ [M + H]$^+$ 415.1302; found, 415.1298.

*3-(3-Hexylureido)thiophene-2-carboxylic Acid (**43**).* A solution of commercially available methyl 3-aminothiophene-2-carboxylate **V** (1.00 g, 6.33 mmol) in H_2O (7.5 mL) and potassium hydroxide (0.63 g, 9.49 mmol, 85%) was heated to 90 °C for 2 h. After full conversion of the starting material, the solution was cooled down to 0 °C and treated with a solution of triphosgene (1.13 g, 3.80 mmol) in THF (7.5 mL). The resulting solution was stirred at room temperature for 4 h, and the residue was filtered. The residue was dissolved in THF (7.5 mL) and treated with hexylamine (1.92 g, 18.99 mmol), and the resulting reaction mixture was stirred at room temperature for 24 h. The precipitate was filtered and washed with cold THF to yield **43** (0.88 g, 3.26 mmol, 51%) as a white amorphous solid.

^{1}H NMR (500 MHz, DMSO-d_6) δ = 0.83−0.90 (m, 3 H), 1.21−1.31 (m, 6 H), 1.35−1.45 (m, 2 H), 3.02−3.09 (m, 2 H), 3.33 (br s, 1 H), 7.58 (br s, 1 H), 7.70 (d, *J* = 5.49 Hz, 1 H), 7.91 (d, *J* = 5.49 Hz, 1 H), 9.27 (br s, 1 H), 12.96 (br s, 1 H). ^{13}C NMR (126 MHz, DMSO-d_6) δ = 13.9, 22.1, 26.1, 29.4, 31.0, 107.0, 121.8, 131.5, 121.8, 131.5, 146,1, 153.8, 165. HRMS (ESI+) *m/z* calculated for $C_{12}H_{19}N_2O_3S$ [M + H]$^+$ 271.1111; found, 271.1108.

*Methyl 3-Amino-4-bromothiophene-2-carboxylate (**VI**).*[23] To a solution of commercially available methyl 3-aminothiophene-2-carboxylate **V** (4.00 g, 25.44 mmol) in acetic acid (30 mL), bromine (4.06 g, 25.44 mmol) was added dropwise. Then, the reaction mixture was stirred at room temperature for 24 h before it was poured into a saturated sodium sulfite solution and extracted with DCM. The organic layer was dried over $MgSO_4$, filtered, and the solvent was removed under reduced pressure. The crude product was purified *via* flash chromatography (SiO_2, petroleum ether/ethyl acetate = 95:5) to yield **VI** (1.92 g, 8.14 mmol, 32%) as a yellow, amorphous solid.

^{1}H NMR (500 MHz, $CDCl_3$) δ = 3.86 (s, 3 H), 5.64 (br s, 2 H), 7.30 (s, 1 H). ^{13}C NMR (126 MHz, $CDCl_3$) δ = 51.5, 100.3, 102.4, 128.0, 150.3, 164.1. HRMS (ESI+) *m/z* calculated for $C_6H_7BrNO_2S$ [M + H]$^+$ 235.9376; found, 235.9373.

*Methyl 3-Amino-4-(3,4-dichlorophenyl)thiophene-2-carboxylate (**VII**).*[25] Methyl 3-amino-4-bromothiophene-2-carboxylate **VI** (0.20 g, 0.85 mmol), (3,4-dichlorophenyl)boronic acid (0.23 g, 1.19 mmol), Na_2CO_3 (0.22 g, 2.11 mmol), and [$Pd(PPh_3)_4$] (48.9 mg, 0.04 mmol) were stirred at 80 °C for 6 h in 1,4-dioxane/H_2O (4:1, 8.5 mL). After complete conversion (TLC), the solution was diluted with ethyl acetate and washed with $KHSO_4$ (1 N) solution and sat. NaCl solution. The organic phase was dried over $MgSO_4$, filtered, and the solvent was removed under reduced pressure. The crude product was purified by column chromatography (SiO_2, petroleum ether/ethyl acetate = 95:5) to yield **VII** (0.23 g, 0.76 mmol, 90%) as a white, amorphous solid.

^{1}H NMR (500 MHz, DMSO-d_6) δ = 3.76 (s, 3 H), 6.39 (s, 2 H), 7.45 (dd, *J* = 8.32, 2.06 Hz, 1 H), 7.70 (d, *J* = 1.98 Hz, 1 H), 7.72 (d, *J* = 8.24 Hz, 1 H), 7.79 (s, 1 H). ^{13}C NMR (126 MHz, DMSO-d_6) δ = 51.2, 99.4, 128.3, 129.9, 130.3, 130.3, 130.9, 131.2, 131.5, 134.6, 152.1, 164.2. HRMS (ESI+) *m/z* calculated for $C_{12}H_{10}Cl_2NO_2S$ [M + H]$^+$ 301.9804; found, 301.9802.

*3-Amino-4-(3,4-dichlorophenyl)thiophene-2-carboxylic Acid (**42**).* To a solution of methyl 3-amino-4-(3,4-dichlorophenyl)-thiophene-2-carboxylate **VII** (151.7 mg, 0.50 mmol) in THF/H_2O (4:1, 5.0 mL), LiOH·H_2O (105.3 mg, 2.51 mmol) was added at 0 °C. After full conversion (TLC), the solvent was evaporated under reduced pressure. The residue was dissolved in H_2O (5.0 mL) and acidified with $KHSO_4$ (1 N) solution. After extraction with DCM (three times), the combined organic phases were dried over Na_2SO_4, filtered, and the solvent was evaporated under vacuum to yield **42** (137.5 mg, 0.48 mmol, 95%) as a white, amorphous solid.

^{1}H NMR (500 MHz, MeOH-d_4) δ = 7.42 (dd, *J* = 8.32, 2.06 Hz, 1 H), 7.50 (s, 1 H), 7.60 (d, *J* = 8.24 Hz, 1 H), 7.66 (d, *J* = 1.98 Hz, 1 H). ^{13}C NMR (126 MHz, MeOH-d_4) δ = 103.5, 129.1, 131.1, 131.2, 132.2, 132.3, 132.7, 134.0, 136.7, 153.1, 167.8. HRMS (ESI+) *m/z* calculated for $C_{11}H_8Cl_2NO_2S$ [M + H]$^+$ 287.9648; found, 287.9644.

*Methyl 4-(3,4-Dichlorophenyl)-3-pentanamidothiophene-2-carboxylic Acid (**VIII**).* To a solution of methyl 3-amino-4-(3,4-dichlorophenyl)thiophene-2-carboxylate **42** (200.0 mg, 0.69 mmol) and DIPEA (107.0 mg, 0.83 mmol) in DCM (7 mL), valeroyl chloride (83.9 mg, 0.69 mmol) was added at −20 °C. The reaction mixture was heated to room temperature overnight, diluted with DCM, and washed successively with $KHSO_4$ (1 N) solution, sat. $NaHCO_3$ solution, and sat. NaCl solution. The solvent was filtered and removed under reduced pressure, and the residue was purified by column chromatography (SiO_2, petroleum ether/ethyl acetate = 80:20). The corresponding amide **VIII** (171.5 mg, 0.44 mmol, 64%) was obtained as a beige, amorphous solid.

^{1}H NMR (500 MHz, $CDCl_3$) δ = 0.91 (t, *J* = 7.40 Hz, 3 H), 1.29−1.37 (m, 2 H), 1.60 (dt, *J* = 15.18, 7.51 Hz, 2 H), 2.31 (t, *J* = 7.55 Hz, 2 H), 3.92 (s, 3 H), 7.25 (d, *J* = 2.14 Hz, 1 H), 7.41−7.46 (m, 2 H), 7.49 (d, *J* = 1.98 Hz, 1 H), 9.00 (br s, 1 H). ^{13}C NMR (126 MHz, $CDCl_3$) δ = 13.7, 22.3, 27.4, 36.9, 52.2, 117.8, 126.0, 128.3, 129.3, 130.5131.3132.5, 136.3, 137.1, 141.0, 163.5, 171.2. HRMS (ESI+) *m/z* calculated for $C_{17}H_{18}Cl_2NO_3S$ [M + H]$^+$ 386.0379; found, 386.0378.

*4-(3,4-Dichlorophenyl)-3-pentanamidothiophene-2-carboxylic Acid (**44**).* To a solution of methyl ester **VIII** (163.6 mg, 0.41 mmol) in THF/H_2O (4:1), LiOH (39.2 mg, 1.63 mmol) was added at 0 °C. After full conversion (TLC), the solvent was evaporated under reduced pressure. The residue was dissolved in H_2O (5 mL) and acidified with $KHSO_4$ (1 N) solution. After extraction with DCM (three times), the combined organic phases were dried over Na_2SO_4, filtered, and the solvent was removed to yield **44** (135.2 mg, 0.36 mmol, 89%) as a white, amorphous solid.

^{1}H NMR (500 MHz, DMSO-d_6) δ = 0.83 (t, *J* = 7.32 Hz, 3 H), 1.20 (dq, *J* = 14.97, 7.52 Hz, 2 H), 1.45 (quin, *J* = 7.40 Hz, 2 H), 2.19 (t, *J* = 7.32 Hz, 2 H), 7.39 (dd, *J* = 8.32, 1.91 Hz, 1 H), 7.64 (d, *J* = 1.83 Hz, 1 H), 7.67 (d, *J* = 8.39 Hz, 1 H), 7.99 (s, 1 H), 9.58 (s, 1 H), 13.21 (br s, 1 H). ^{13}C NMR (126 MHz, DMSO-d_6) δ = 13.8, 21.8, 27.1, 35.3, 126.2, 127.8, 128.9, 129.1, 130.1, 130.7, 131.1, 135.6,

https://doi.org/10.1021/acs.jmedchem.1c02114
J. Med. Chem. 2022, 65, 8869−8880

138.1, 138.5, 162.3, 171.8. HRMS (ESI+) m/z calculated for $C_{16}H_{16}Cl_2NO_3S$ $[M + H]^+$ 372.0223; found, 372.0219.

*Methyl 4-(3,4-Dichlorophenyl)-3-(hexylamino)thiophene-2-carboxylate (**IX**).* Sodium hydride (90% mineral oil dispersion, 24.8 mg, 0.94 mmol) was added to a solution of methyl 3-amino-4-(3,4-dichlorophenyl)thiophene-2-carboxylate **VII** (0.26 g, 0.85 mmol) in dry DMF (6 mL) at 0 °C. After 1 h, 1-bromophexane (0.14 g, 0.85 mmol) was added, and the reaction mixture was stirred at room temperature for 12 h, poured into ice water, and extracted with ethyl acetate (three times). The combined organic layers were washed with sat. NaCl solution, dried over $MgSO_4$, filtered, and concentrated under vacuum. The crude product was purified by flash chromatography (SiO_2, petroleum ether/ethyl acetate = 98:2) to yield **IX** (0.22 g, 0.57 mmol, 67%) as a yellow oil.

^{1}H NMR (500 MHz, $CDCl_3$) δ = 0.84 (t, J = 7.25 Hz, 3 H), 1.10–1.18 (m, 4 H), 1.19–1.27 (m, 2 H), 1.35–1.42 (m, 2 H), 2.78 (t, J = 7.02 Hz, 2 H), 3.86 (s, 3 H), 6.81 (br s, 1 H), 7.21 (s, 1 H), 7.30–7.36 (m, 1 H), 7.47 (d, J = 8.24 Hz, 1 H), 7.58 (d, J = 1.98 Hz, 1 H). ^{13}C NMR (126 MHz, $CDCl_3$) δ = 14.0, 22.5, 26.2, 30.5, 31.4, 46.7, 51.4, 105.1, 127.6, 130.0, 130.3, 131.0, 131.6, 132.0, 132.5, 136.4, 154.5, 165.1. HRMS (ESI+) m/z calculated for $C_{18}H_{22}Cl_2NO_2S$ $[M + H]^+$ 386.0743; found, 386.0738.

*4-(3,4-Dichlorophenyl)-3-(hexylamino)thiophene-2-carboxylic Acid (**45**).* To a solution of methyl ester **IX** (176.7 mg, 0.47 mmol) in THF/H_2O (4:1) (2.4 mL), LiOH·H_2O (95.9 mg, 2.29 mmol) was added at 0 °C. After full conversion (TLC), the solvent was evaporated under reduced pressure. The residue was dissolved in H_2O (5 mL) and acidified with $KHSO_4$ (1 N) solution. After extraction with DCM (three times), the combined organic phases were dried over Na_2SO_4, filtered, and the solvent was removed. The acid **45** (160.4 mg, 0.43 mmol, 91%) could be obtained as a brown oil.

^{1}H NMR (500 MHz, DMSO-d_6) δ = 0.79 (t, J = 7.25 Hz, 3 H), 1.02–1.11 (m, 4 H), 1.11–1.19 (m, 2 H), 1.22–1.31 (m, 3 H), 2.71 (br t, J = 6.87 Hz, 2 H), 6.68–6.84 (m, 1 H), 7.46 (dd, J = 8.24, 1.98 Hz, 1 H), 7.69 (d, J = 8.24 Hz, 1 H) 7.72 (d, J = 1.98 Hz, 1 H), 7.74 (s, 1 H) 12.74 (br s, 1 H). ^{13}C NMR (126 MHz, DMSO-d_6) δ = 13.9, 22.0, 25.6, 29.9, 30.7, 45.9, 105.7, 128.3, 129.7, 130.1, 130.6, 131.2, 131.5, 131.9, 136.7, 154.0, 165.6. HRMS (ESI+) m/z calculated for $C_{16}H_{20}Cl_2NS$ [M-COOH + 2H]$^+$ 328.0688; found, 328.0685.

*Methyl 2-Amino-3′,4′-dichloro-[1,1′-biphenyl]-3-carboxylate (**XI**).*[24] Methyl 2-amino-3-bromobenzoate **X** (0.20 g, 0.87 mmol), (3,4-dichlorophenyl)boronic acid (0.23 g, 1.21 mmol), Na_2CO_3 (0.22 g, 2.11 mmol), and $[Pd(PPh_3)_4]$ (50.2 mg, 0.04 mmol) were stirred at 80 °C for 6 h in 8.5 mL of 1,4-dioxane/H_2O (4:1). After complete conversion (TLC), the solution was diluted with ethyl acetate and washed with $KHSO_4$ (1 N) solution and sat. NaCl solution. The organic phase was dried over $MgSO_4$, filtered, and the solvent was removed under reduced pressure. The crude product was purified by column chromatography (SiO_2, petroleum ether/ethyl acetate = 98:2) to yield **XI** (0.17 g, 0.56 mmol, 65%) as a white, amorphous solid.

^{1}H NMR (500 MHz, $CDCl_3$) δ = 3.90 (s, 3 H), 6.72 (t, J = 7.71 Hz, 1 H), 7.18 (dd, J = 7.32, 1.53 Hz, 1 H), 7.28–7.30 (m, 1 H), 7.53 (s, 1 H), 7.54 (d, J = 8.11 Hz, 1 H), 7.93 (dd, J = 8.09, 1.68 Hz, 1 H). ^{13}C NMR (126 MHz, $CHCl_3$-d) δ = 51.8, 111.1, 116.0, 126.2, 128.7, 131.0, 131.3, 131.5, 131.9, 133.1, 134.9, 138.5, 147.5, 168.6. HRMS (ESI+) m/z calculated for $C_{14}H_{12}Cl_2NO_2$ $[M + H]^+$ 296.0240; found, 296.0237.

*2-Amino-3′,4′-dichloro-[1,1′-biphenyl]-3-carboxylic Acid (**XII**).* To a solution of methyl ester **XI** (163.7 mg, 0.55 mmol) in THF/H_2O (4:1) (2.8 mL), LiOH (66.1 mg, 2.76 mmol) was added at 0 °C. After full conversion (TLC), the solvent was evaporated under reduced pressure. The residue was dissolved in H_2O (5 mL) and acidified with $KHSO_4$ (1 N) solution. After extraction with DCM (three times), the combined organic phases were dried over Na_2SO_4 and filtered, and the solvent was removed under reduced pressure to obtain **XII** (151.2 mg, 0.54 mmol, 97%) as a white, amorphous solid.

^{1}H NMR (500 MHz, DMSO-d_6) δ = 6.64 (t, J = 7.71 Hz, 1 H), 7.19 (dd, J = 7.32, 1.68 Hz, 1 H), 7.38 (dd, J = 8.24, 1.98 Hz, 1 H), 7.63 (d, J = 2.14 Hz, 1 H), 7.71 (d, J = 8.24 Hz, 1 H), 7.80 (d, J = 7.93 Hz, 1 H). ^{13}C NMR (126 MHz, DMSO-d_6) δ = 110.6, 115.0, 125.6, 129.7, 130.1, 131.1, 131.2, 131.5, 131.7, 135.1, 139.3, 148.3, 169.8. HRMS (ESI+) m/z calculated for $C_{13}H_{10}Cl_2NO_2$ $[M + H]^+$ 282.0083; found, 282.0079.

*3′,4′-Dichloro-2-(3-hexylureido)-[1,1′-biphenyl]-3-carboxylic Acid (**46**).* To a stirred solution of acid **XII** (149.7 mg, 0.53 mmol) in THF (5.3 mL), triphosgene (94.5 mg, 0.32 mmol) was added. The reaction mixture was stirred for 2 h at room temperature before treating carefully with saturated $NaHCO_3$ solution (5.3 mL). After extraction with ethyl acetate (three times), the combined organic layers were washed with sat. NaCl solution, dried over $MgSO_4$, and the solvent was filtered and removed concentrated under vacuum. The obtained residue was dissolved in THF (5.3 mL) and H_2O (5.3 mL) before hexylamine (107.3 mg, 1.06 mmol) was added. After stirring at room temperature for 24 h, the reaction mixture was poured into ice-cooled HCl (2 N) (20 mL) and extracted with ethyl acetate (three times). The organic layers were washed with HCl (2 N) (20 mL) and sat. NaCl solution, dried over $MgSO_4$, filtered, and concentrated under vacuum. The crude product was purified by preparative HPLC to yield **46** (83.0 mg, 0.20 mmol, 38%) as a white, amorphous solid.

^{1}H NMR (500 MHz, DMSO-d_6) δ = 0.86 (t, J = 6.87 Hz, 3 H), 1.07–1.20 (m, 6 H), 1.20–1.32 (m, 3 H), 2.73–2.88 (m, 2 H), 6.75 (br s, 1 H), 7.25 (t, J = 7.48 Hz, 1 H), 7.32 (d, J = 7.78 Hz, 1 H), 7.45 (d, J = 7.17 Hz, 1 H), 7.57 (br s, 1 H), 7.61 (d, J = 8.24 Hz, 1 H), 7.82 (d, J = 7.48 Hz, 1 H), 8.57 (br s, 1 H), 13.19 (br s, 1 H). ^{13}C NMR (126 MHz, DMSO-d_6) δ = 14.1, 22.1, 25.9, 29.7, 31.1, 123.9, 125.6, 128.6, 129.2, 129.9, 130.1, 130.3, 130.7, 134.0, 135.4, 137.3, 141.0, 154.6, 168.6. HRMS (ESI+) m/z calculated for $C_{20}H_{23}Cl_2N_2O_3$ $[M + H]^+$ 409.1080; found, 409.1076.

*Methyl 3-Amino-4-(2,5-dichlorophenyl)thiophene-2-carboxylate (**XIII**).* Methyl 3-amino-4-bromothiophene-2-carboxylate (**VI**) (0.20 g, 0.85 mmol), (2,5-dichlorophenyl)boronic acid (0.23 g, 1.19 mmol), Na_2CO_3 (0.22 g, 2.11 mmol), and $[Pd(PPh_3)_4]$(48.9 mg, 0.04 mmol) were stirred at 80 °C for 6 h in 1,4-dioxane/H_2O (4:1) (8.5 mL). After complete conversion (TLC), the solution was diluted with ethyl acetate and washed with $KHSO_4$ (1 N) solution and sat. NaCl solution. The organic phase was dried over $MgSO_4$ and filtered, and the solvent was removed under reduced pressure. The crude product was purified by column chromatography (SiO_2, petroleum ether/ethyl acetate = 95:5) to yield **XIII** (0.24 g, 0.79 mmol, 93%) as a white, amorphous solid.

^{1}H NMR (500 MHz, $CDCl_3$) δ = 3.86 (s, 3 H), 5.43 (br s, 2 H), 7.28 (s, 1 H), 7.30–7.34 (m, 1 H), 7.35 (d, J = 2.44 Hz, 1 H), 7.44 (d, J = 8.54 Hz, 1 H). ^{13}C NMR (126 MHz, $CDCl_3$) δ = 51.4, 116.7, 121.5, 129.0, 129.8, 130.7, 131.2, 131.5, 132.2, 133.0, 134.3, 151.4, 164.9. HRMS (ESI+) m/z calculated for $C_{12}H_{10}Cl_2NO_2S$ $[M + H]^+$ 301.9804; found, 301.9799.

*3-Amino-4-(2,5-dichlorophenyl)thiophene-2-carboxylic Acid (**XIV**).* To a solution of methyl 3-amino-4-(2,5-dichlorophenyl)-thiophene-2-carboxylate(**XIII**) (221.8 mg, 0.73 mmol) in THF/H_2O (4:1) (7.3 mL), LiOH·H_2O (153.2 mg, 3.65 mmol) was added at 0 °C. After full conversion (TLC), the solvent was evaporated under reduced pressure. The residue was dissolved in H_2O (5 mL) and acidified with $KHSO_4$ (1 N) solution. After extraction with DCM (three times), the combined organic phases were dried over Na_2SO_4, filtered, and the solvent was evaporated under vacuum to yield **XIV** (188.9 mg, 0.66 mmol, 90%) as a white, amorphous solid.

^{1}H NMR (500 MHz, DMSO-d_6) δ = 2.52–2.57, (m, 1 H), 5.84–6.53 (m, 1 H), 7.44 (d, J = 2.59 Hz, 1 H), 7.51 (dd, J = 8.62, 2.52 Hz, 1 H), 7.61 (d, J = 8.70 Hz, 1 H), 7.63 (s, 1 H), 11.40–12.88 (m, 1 H). ^{13}C NMR (126 MHz, DMSO-d_6) δ = 128.9, 129.7, 131.2, 131.3, 131.6, 131.8, 132.0, 134.8, 152.3, 165.5. HRMS (ESI+) m/z calculated for $C_{11}H_8Cl_2NO_2S$ $[M + H]^+$ 287.9647; found, 287.9641.

*3-(3-Butyl-3-phenylureido)-4-(2,5-dichlorophenyl)thiophene-2-carboxylic Acid (**47**).* To a stirred solution of acid **XIV** (188.2 mg, 0.65 mmol) in THF (6.5 mL), triphosgene (139.5 mg, 0.47 mmol) was added. The reaction mixture was stirred for 2 h at room temperature before careful treatment with saturated $NaHCO_3$ solution (5.3 mL). After extraction with ethyl acetate (three times), the combined organic layers were washed with sat. NaCl solution,

https://doi.org/10.1021/acs.jmedchem.1c02114
J. Med. Chem. 2022, 65, 8869–8880

dried over $MgSO_4$, and the solvent was filtered and removed by a vacuum. The obtained residue was dissolved in THF (6.5 mL) and H_2O (6.5 mL) before *N*-butylaniline (213.4 mg, 1.43 mmol) was added. After stirring at room temperature for 24 h, the reaction mixture was poured into ice-cooled HCl (2 N) (20 mL) and extracted with ethyl acetate (three times). The organic layers were washed with HCl (2 N) (20 mL) and sat. NaCl solution, dried over $MgSO_4$, filtered, and concentrated in vacuum. The crude product was purified by preparative HPLC to yield **47** (41.4 mg, 0.09 mmol, 14%) as a white, amorphous solid.

^{1}H NMR (500 MHz, DMSO-d_6) δ = 0.73 (t, *J* = 7.25 Hz, 3 H), 1.04 (sxt, *J* = 7.39 Hz, 2 H), 1.13−1.23 (m, 2 H), 3.41−3.44 (m, 2 H), 7.28−7.32 (m, 2 H), 7.36−7.42 (m, 3 H), 7.47−7.52 (m, 2 H), 7.54 (d, *J* = 8.54 Hz, 1 H), 7.84−7.86 (m, 1 H), 8.38 (s, 1 H). ^{13}C NMR (126 MHz, DMSO-d_6) δ = 13.7, 18.9, 29.5, 48.1, 114.8, 127.8128.3, 128.4, 129.9, 130.5, 130.9, 131.3, 131.4, 133.4, 137.2, 140.9, 143.2, 152.2, 164.4. HRMS (ESI+) *m*/*z* calculated for $C_{22}H_{21}Cl_2N_2O_3S$ $[M + H]^+$ 463.0644; found, 463.0638.

Methyl 3-Amino-4-(4-phenoxyphenyl)thiophene-2-carboxylate (XV). Methyl 3-amino-4-bromothiophene-2-carboxylate (**VI**) (0.20 g, 0.85 mmol), (4-phenoxyphenyl)boronic acid (0.25 g, 1.19 mmol), Na_2CO_3 (0.22 g, 2.11 mmol), and $[Pd(PPh_3)_4]$ (48.9 mg, 0.04 mmol) were stirred at 80 °C for 6 h in 1,4-dioxane/H_2O (4:1) (8.5 mL). After complete conversion (TLC), the solution was diluted with ethyl acetate and washed with $KHSO_4$ (1 N) solution and sat. NaCl solution. The organic phase was dried over $MgSO_4$, filtered, and the solvent was removed under reduced pressure. The crude product was purified by column chromatography (SiO_2, petroleum ether/ethyl acetate = 95:5) to yield **XV** (0.22 g, 0.68 mmol, 80%) as a white, amorphous solid.

^{1}H NMR (500 MHz, $CDCl_3$) δ = 3.87 (s, 3 H), 5.63 (br s, 2 H), 7.06−7.10 (m, 4 H), 7.16 (t, *J* = 7.42 Hz, 1 H), 7.22 (s, 1 H), 7.36−7.42 (m, 4 H). ^{13}C NMR (126 MHz, $CDCl_3$) δ = 51.3, 101.3, 119.0, 119.3, 123.7, 128.4, 129.1, 129.5, 129.9, 132.7, 151.5, 156.6, 157.3, 165.1. HRMS (ESI+) *m*/*z* calculated for $C_{18}H_{16}NO_3S$ $[M + H]^+$ 326.0845; found, 326.0839.

3-Amino-4-(4-phenoxyphenyl)thiophene-2-carboxylic Acid (XVI). To a solution of methyl 3-amino-4-(4-phenoxyphenyl)-thiophene-2-carboxylate (**XV**) (197.4 mg, 0.60 mmol) in THF/H_2O (4:1) (6.0 mL), LiOH·H_2O (122.2 mg, 2.91 mmol) was added at 0 °C. After full conversion (TLC), the solvent was evaporated under reduced pressure. The residue was dissolved in H_2O (5.0 mL) and acidified with $KHSO_4$ (1 N) solution. After extraction with DCM (three times), the combined organic phases were dried over Na_2SO_4, filtered, and the solvent was evaporated under vacuum to yield **XVI** (176.1 mg, 0.57 mmol, 94%) as a white, amorphous solid.

^{1}H NMR (500 MHz, DMSO-d_6) δ = 6.00−6.62 (m, 1 H), 7.04−7.11 (m, 4 H), 7.17 (t, *J* = 7.41 Hz, 1 H), 7.39−7.45 (m, 2 H), 7.45−7.50 (m, 1 H), 7.45−7.49 (m, 1 H), 7.58 (s, 1 H). ^{13}C NMR (126 MHz, DMSO-d_6) δ = 100.4, 118.8, 118.9, 123.7, 128.9, 129.5, 129.6, 130.1, 132.3, 151.9, 156.3, 156.4, 165.6. HRMS (ESI+) *m*/*z* calculated for $C_{17}H_{14}NO_3S$ $[M + H]^+$ 312.0689; found, 312.0681.

3-(3-Butyl-3-phenylureido)-4-(4-phenoxyphenyl)thiophene-2-carboxylic Acid (48). To a stirred solution of acid **XVI** (192.8 mg, 0.62 mmol) in THF (6.2 mL), triphosgene (132.3 mg, 0.44 mmol) was added. The reaction mixture was stirred at room temperature for 2 h before treating carefully with saturated $NaHCO_3$ solution (6.2 mL). After extraction with ethyl acetate (three times), the combined organic layers were washed with sat. NaCl solution, dried over $MgSO_4$, filtered, and the solvent was removed under vacuum. The obtained residue was dissolved in THF (6.2 mL) and H_2O (6.2 mL) before *N*-butylaniline (203.5 mg, 1.36 mmol) was added. After stirring for 24 h at room temperature, the reaction mixture was poured into ice-cooled HCl (2 N) (20 mL) and extracted with ethyl acetate (three times). The organic layers were washed with HCl (2 N) (20 mL) and sat. NaCl solution, dried over $MgSO_4$, filtered, and concentrated in vacuum. The crude product was purified by preparative HPLC to yield **48** (41.6 mg, 0.09 mmol, 14%) as a white, amorphous solid.

^{1}H NMR (500 MHz, DMSO-d_6) δ = 0.75 (t, *J* = 7.32 Hz, 3 H, H-29), 1.16 (sxt, *J* = 7.35 Hz, 2 H, H-28), 1.22−1.32 (m, 2 H, H-27) 3.48 (t, *J* = 7.10 Hz, 2 H, H-26), 7.03 (d, *J* = 7.93 Hz, 2 H, H-21, H-22), 7.04−7.07 (m, 2 H, H-7, H-8), 7.16 (t, *J* = 7.40 Hz, 1 H, H-18), 7.35 (d, *J* = 7.32 Hz, 2 H, H-13, H-14), 7.38 (br d, *J* = 7.48 Hz, 1 H, H-25), 7.41 (t, *J* = 7.93 Hz, 2 H, H-16, H-17), 7.45 (d, *J* = 8.54 Hz, 2 H, H-9, H-10), 7.47−7.51 (m, 2 H, H-23, H-24), 7.75 (s, 1 H, H-5), 8.09 (br s, 1 H, NH), 13.22 (br s, 1 H, COOH). ^{13}C NMR (126 MHz, DMSO-d_6) δ = 13.7 (C-29), 19.1 (C-28), 29.8 (C-27), 48.3 (C-26), 118.5 (C-21), 118.6 (C-22), 123.5 (C-18), 127.5 (C-25), 127.8 (C-5), 128.1 (C-9, C-10), 128.3 (C-14, C-15), 129.7 (C-23, C-24), 129.9 (C-16, C-17), 131.6 (C-6), 138.1 (C-3), 141.3 (C-2), 142.4 (C-4), 152.9 (C-20), 155.5 (C-12), 156.8 (C-13), 164.2 (C-1). HRMS (ESI+) *m*/*z* calculated for $C_{28}H_{27}N_2O_4S$ $[M + H]^+$ 487.1686; found, 487.1680.

■ ASSOCIATED CONTENT

Supporting Information

The Supporting Information is available free of charge at https://pubs.acs.org/doi/10.1021/acs.jmedchem.1c02114.

Molecular formula strings (CSV)

^{1}H NMR and ^{13}C NMR spectra, HPLC data, biological assays, and structure-based virtual screening (PDF)

■ AUTHOR INFORMATION

Corresponding Author

Anna K.H. Hirsch − *Helmholtz-Institute for Pharmaceutical Research Saarland (HIPS)−Helmholtz Centre for Infection Research (HZI), 66123 Saarbrücken, Germany; Department of Pharmacy, Saarland University, 66123 Saarbrücken, Germany; Helmholtz International Lab for Anti-Infectives, 66123 Saarbrücken, Germany*; orcid.org/0000-0001-8734-4663; Email: anna.hirsch@helmholtz-hips.de

Authors

Alexander F. Kiefer − *Helmholtz-Institute for Pharmaceutical Research Saarland (HIPS)−Helmholtz Centre for Infection Research (HZI), 66123 Saarbrücken, Germany*; orcid.org/0000-0002-4540-6501

Spyridon Bousis − *Helmholtz-Institute for Pharmaceutical Research Saarland (HIPS)−Helmholtz Centre for Infection Research (HZI), 66123 Saarbrücken, Germany; Department of Pharmacy, Saarland University, 66123 Saarbrücken, Germany*

Mostafa M. Hamed − *Helmholtz-Institute for Pharmaceutical Research Saarland (HIPS)−Helmholtz Centre for Infection Research (HZI), 66123 Saarbrücken, Germany*; orcid.org/0000-0002-7374-6992

Eleonora Diamanti − *Helmholtz-Institute for Pharmaceutical Research Saarland (HIPS)−Helmholtz Centre for Infection Research (HZI), 66123 Saarbrücken, Germany; Helmholtz International Lab for Anti-Infectives, 66123 Saarbrücken, Germany*

Jörg Haupenthal − *Helmholtz-Institute for Pharmaceutical Research Saarland (HIPS)−Helmholtz Centre for Infection Research (HZI), 66123 Saarbrücken, Germany*

Complete contact information is available at: https://pubs.acs.org/10.1021/acs.jmedchem.1c02114

Author Contributions

[‖]A.F.K., S.B., and M.M.H. contributed equally. Alexander F. Kiefer contributed to the conception of this study, designed and performed experiments, and evaluated and interpreted resulting data. The author developed the synthetic route, performed the synthesis experiments and chemical analysis of

the compounds, as well as contributed to the writing and editing of the manuscript. Spyridon Bousis contributed to the conception of this study, designed and performed the virtual screening, evaluated and interpreted resulting data, as well as contributed to the writing and editing of the manuscript. Mostafa M. Hamed contributed to the design and conception of this study, evaluated and interpreted resulting data, as well as contributed to the writing and editing of the manuscript. Additionally, the author coordinated the ECF bioassays. Eleonora Diamanti contributed to the conception of this study, designed and performed the virtual screening, evaluated and interpreted resulting data, and edited and proofread the manuscript. Jörg Haupenthal contributed to editing and proofreading of the manuscript and coordination of the solubility, antimicrobial, and cytotoxicity assays. Anna K.H. Hirsch contributed to the conception of the study, supervised this study, as well as contributed to the editing and proofreading of the manuscript.

Funding

A.K.H.H. gratefully acknowledges funding from the Netherlands Organization for Scientific Research (ChemThem and VIDI grants). A.K.H.H. acknowledges funding from the European Research Council (ERC starting grant 757913), the European Union's Horizon 2020 research and innovation program under Marie Skłodowska Curie grant agreement no. 665250, and the Helmholtz-Association's Initiative and Networking Fund.

Notes

The authors declare no competing financial interest.

■ ACKNOWLEDGMENTS

We thank Andreas M. Kany and Selina Wolter for performing kinetic solubility assays. Additionally, we thank Jeannine Jung, Stefanie Schmitt, and Alexandra Amann for performing the ECF bioassays and MIC determination of Gram-positive pathogens, which were coordinated by Dr. Jennifer Herrmann and Prof. Rolf Müller.

■ ABBREVIATIONS

ABC, ATP-binding cassette; AMR, antimicrobial resistance; ATP, adenosine 5′-triphosphate; ECF, energy-coupling factor; *E. faecalis*, *Enterococcus faecalis*; *E. faecium*, *Enterococcus faecium*; IC_{50}, half-maximal inhibitory concentration; HPLC, high−performance liquid chromatography; *L. casei*, *Lactobacillus casei*; MIC, minimum inhibitory concentration; MDR, multidrug resistant; NBD, nucleotide-binding domain; PR, penicillin-resistant; *S. aureus*, *Staphylococcus aureus*; *S. pneumoniae*, *Streptococcus pneumoniae*; SAR, structure−activity relationship; BTC, triphosgene; VR, vancomycin-resistant

■ REFERENCES

(1) Ahmed, Y. A.; Anand, B.; Hanan Hassan, A. B.; Banerjee, S.; Bertagnolio, S.; Bruinsma, N.; Cavallier, P.; Chowdary, T.; Dean, A.; El Olmeri, N.; Eraly, E.; Escalante, S.; Escher, M.; Fuller, W.; Gahimbare, L.; Gelormini, M.; Giron, A. C.; Glaziou, P.; Gordon, B. A.; Ivanovska, V.; Iwamoto, K.; Jung, T. R.; Wong, D. L. F.; Matheu, J. R.; Alvarez, K. O. M.; Muller, A.; Nishijima, T.; O'Doherty, D.; Ramon-Pardo, P.; Rasmussen, C.; Ringwald, P.; Siswanto, S.; Lorenzo Subissi, M.; Ismail, T.; Tosas, O.; Van Weezenbeek, C.; Vong, S.; Wi, T. E.; Zamora, D. M.; Zayed, B. *Global Antimicrobial Resistance and Use Surveillance System (GLASS) Report 2021*; 2021.

(2) Theuretzbacher, U.; Bush, K.; Harbarth, S.; Paul, M.; Rex, J. H.; Tacconelli, E.; Thwaites, G. E. Critical Analysis of Antibacterial Agents in Clinical Development. *Nat. Rev. Microbiol.* **2020**, *18*, 286−298.

(3) Rempel, S.; Stanek, W. K.; Slotboom, D. J. ECF-Type ATP-Binding Cassette Transporters. *Annu. Rev. Biochem.* **2019**, *88*, 551−576.

(4) Henderson, G. B.; Huennekens, F. M. Transport of Folate Compounds into Lactobacillus Casei. *Arch. Biochem. Biophys.* **1974**, *728*, 722−728.

(5) Zhang, M.; Bao, Z.; Zhao, Q.; Guo, H.; Xu, K.; Wang, C.; Zhang, P. Structure of a Pantothenate Transporter and Implications for ECF Module Sharing and Energy Coupling of Group II ECF Transporters. *Proc. Natl. Acad. Sci. U. S. A.* **2014**, *111*, 18560−18565.

(6) Karpowich, N. K.; Song, J.; Wang, D. N. An Aromatic Cap Seals the Substrate Binding Site in an ECF-Type S Subunit for Riboflavin. *J. Mol. Biol.* **2016**, *428*, 3118−3130.

(7) Bao, Z.; Qi, X.; Hong, S.; Xu, K.; He, F.; Zhang, M.; Chen, J.; Chao, D.; Zhao, W.; Li, D.; Wang, J.; Zhang, P. Structure and Mechanism of a Group-I Cobalt Energy Coupling Factor Transporter. *Cell Res.* **2017**, *27*, 675−687.

(8) Rodionov, D. A.; Hebbeln, P.; Gelfand, M. S.; Eitinger, T. Comparative and Functional Genomic Analysis of Prokaryotic Nickel and Cobalt Uptake Transporters: Evidence for a Novel Group of ATP-Binding Cassette Transporters. *J. Bacteriol.* **2006**, *188*, 317−327.

(9) Rodionov, D. A.; Hebbeln, P.; Eudes, A.; Ter Beek, J.; Rodionova, I. A.; Erkens, G. B.; Slotboom, D. J.; Gelfand, M. S.; Osterman, A. L.; Hanson, A. D.; Eitinger, T. A Novel Class of Modular Transporters for Vitamins in Prokaryotes. *J. Bacteriol.* **2009**, *191*, 42−51.

(10) Henderson, G. B.; Zevely, E. M.; Huennekens, F. M. Mechanism of Folate Transport in Lactobacillus Casei: Evidence for a Component Shared with the Thiamine and Biotin Transport Systems. *J. Bacteriol.* **1979**, *137*, 1308−1314.

(11) Swier, L. J. Y. M.; Guskov, A.; Slotboom, D. J. Structural Insight in the Toppling Mechanism of an Energy-Coupling Factor Transporter. *Nat. Commun.* **2016**, *7*, DOI: 10.1038/ncomms11072.

(12) Bousis, S.; Setyawati, I.; Diamanti, E.; Slotboom, D. J.; Hirsch, A. K. H. Energy-Coupling Factor Transporters as Novel Antimicrobial Targets. *Adv. Ther.* **2019**, *2*, 1800066.

(13) Diamanti, E.; Setyawati, I.; Bousis, S.; Souza, P. C. T.; Gómez, L. M.; Swier, L. J. Y. M.; Haupenthal, J.; Gibson, P. S.; Volz, C.; Stanek, W. K.; Jäger, M.; Herrmann, J.; Marrink, S. J.; Veening, J.-W.; Müller, R.; Slotboom, D. J.; Hirsch, A. K. H. Targeting the Energy-Coupling Factor (ECF) Transporters: Identification of New Tool Compounds. *ChemRxiv* **2021**, DOI: 10.26434/chemrxiv-2021-xq08b-v2.

(14) Bousis, S.; Winkler, S.; Haupenthal, J.; Fulco, F.; Diamanti, E.; Hirsch, A. K. H. An Efficient Way to Screen Inhibitors of Energy-Coupling Factor (ECF) Transporters in a Bacterial Uptake Assay. *Int. J. Mol. Sci.* **2022**, *23*, 2637.

(15) Goddard, T. D.; Huang, C. C.; Ferrin, T. E. Software Extensions to UCSF Chimera for Interactive Visualization of Large Molecular Assemblies. *Structure* **2005**, *13*, 473−482.

(16) Elgaher, W. A. M.; Fruth, M.; Groh, M.; Haupenthal, J.; Hartmann, R. W. Expanding the Scaffold for Bacterial RNA Polymerase Inhibitors: Design, Synthesis and Structure-Activity Relationships of Ureido-Heterocyclic-Carboxylic Acids. *RSC Adv.* **2013**, *4*, 2177−2194.

(17) Sahner, J. H.; Empting, M.; Kamal, A.; Weidel, E.; Groh, M.; Börger, C.; Hartmann, R. W. Exploring the Chemical Space of Ureidothiophene-2-Carboxylic Acids as Inhibitors of the Quorum Sensing Enzyme PqsD from Pseudomonas Aeruginosa. *Eur. J. Med. Chem.* **2015**, *96*, 14−21.

(18) Sahner, J. H.; Groh, M.; Negri, M.; Haupenthal, J.; Hartmann, R. W. Novel Small Molecule Inhibitors Targeting the "Switch Region" of Bacterial RNAP: Structure-Based Optimization of a Virtual Screening Hit. *Eur. J. Med. Chem.* **2013**, *65*, 223−231.

(19) Hartmann, H.; Liebscher, J. A Simple Method for the Synthesis of 5-Aryl-3-Amino-2-Alkoxycarbonylthiophenes. *Synthesis* **1984**, *1984*, 275−276.

(20) Le Foulon, F. X.; Braud, E.; Fabis, F.; Lancelot, J. C.; Rault, S. Synthesis and Combinatorial Approach of the Reactivity of 6- and 7-Arylthieno[3,2-d][1,3]Oxazine-2,4-Diones. *Tetrahedron* **2003**, *59*, 10051−10057.
(21) Fabis, F.; Jolivet-Fouchet, S.; Robba, M.; Landelle, H.; Rault, S. Thiaisatoic Anhydrides : Efficient Synthesis under Microwave Heating Conditions and Study of Their Reactivity. *Tetrahedron* **1998**, *54*, 10789−10800.
(22) Le Foulon, F. X.; Braud, E.; Fabis, F.; Lancelot, J. C.; Rault, S. Solution-Phase Parallel Synthesis of a 1140-Member Ureidothiophene Carboxylic Acid Library. *J. Comb. Chem.* **2005**, *7*, 253−257.
(23) Qian, H. Y.; Wang, Z. L.; Chen, L. L.; Pan, Y. L.; Xie, X. Y.; Xie, X.; Chen, J. Z. Design, Synthesis, and SAR Studies of Heteroarylpyrimidines and Heteroaryltriazines as CB2R Ligands. *ChemMedChem* **2018**, *13*, 2455−2463.
(24) Yamada, K.; Nakazawa, M.; Matsumoto, K.; Tagami, U.; Hirokawa, T.; Homma, K.; Mori, S.; Matsumoto, R.; Saikawa, W.; Kitajima, S. Unnatural Tripeptides as Potent Positive Allosteric Modulators of T1R2/T1R3. *ACS Med. Chem. Lett.* **2019**, *10*, 800−805.
(25) Thalji, R. K.; Raha, K.; Andreotti, D.; Checchia, A.; Cui, H.; Meneghelli, G.; Profeta, R.; Tonelli, F.; Tommasi, S.; Bakshi, T.; Donovan, B. T.; Howells, A.; Jain, S.; Nixon, C.; Quinque, G.; McCloskey, L.; Bax, B. D.; Neu, M.; Chan, P. F.; Stavenger, R. A. Structure-Guided Design of Antibacterials That Allosterically Inhibit DNA Gyrase. *Bioorg. Med. Chem. Lett.* **2019**, *29*, 1407−1412.
(26) Schütz, C.; Ho, D. K.; Hamed, M. M.; Abdelsamie, A. S.; Röhrig, T.; Herr, C.; Kany, A. M.; Rox, K.; Schmelz, S.; Siebenbürger, L.; Wirth, M.; Börger, C.; Yahiaoui, S.; Bals, R.; Scrima, A.; Blankenfeldt, W.; Horstmann, J. C.; Christmann, R.; Murgia, X.; Koch, M.; Berwanger, A.; Loretz, B.; Hirsch, A. K. H.; Hartmann, R. W.; Lehr, C. M.; Empting, M. A New PqsR Inverse Agonist Potentiates Tobramycin Efficacy to Eradicate Pseudomonas Aeruginosa Biofilms. *Adv. Sci.* **2021**, *8*, 1−12.
(27) Lascelles, J.; Woods, D. D. The Synthesis of Folic Acid by Bacterium Coll and Staphylococcus Aureus and Its Inhibition by Sulphonamides. *Br. J. Exp. Pathol.* **1952**, *33*, 288−303.

https://doi.org/10.1021/acs.jmedchem.1c02114
J. Med. Chem. 2022, 65, 8869−8880